

ClassPruning: Speed Up Image Restoration Networks by Dynamic $N:M$ Pruning

Yang Zhou[†] Yuda Song[†] Hui Qian Xin Du[✉]
 Zhejiang University, Hangzhou, China
 {yang_zhou, syd, qianhui, duxin}@zju.edu.cn

Abstract

Image restoration tasks have achieved tremendous performance improvements with the rapid advancement of deep neural networks. However, most prevalent deep learning models perform inference statically, ignoring that different images have varying restoration difficulties and lightly degraded images can be well restored by slimmer subnetworks. To this end, we propose a new solution pipeline dubbed *ClassPruning* that utilizes networks with different capabilities to process images with varying restoration difficulties. In particular, we use a lightweight classifier to identify the image restoration difficulty, and then the sparse subnetworks with different capabilities can be sampled based on predicted difficulty by performing dynamic $N:M$ fine-grained structured pruning on base restoration networks. We further propose a novel training strategy along with two additional loss terms to stabilize training and improve performance. Experiments demonstrate that *ClassPruning* can help existing methods save approximately 40% FLOPs while maintaining performance.

1. Introduction

Image restoration aims to reconstruct high-quality clean images from low-quality inputs corrupted by various degradations. Due to the ill-posed nature, obtaining the optimal result in the infinite solution space is highly challenging. Recently, deep neural networks (DNNs) have developed rapidly and gradually become a preferred alternative to conventional restoration methods. Its strong capability to restore degraded images has been witnessed in various image restoration tasks, including image denoising [49, 58], deraining [38, 61], deblurring [6, 62], dehazing [39, 55], etc.

Despite the remarkable success, high-capacity image restoration networks tend to be quite complex, resulting in significant inference costs, especially when used on mobile devices with limited computational resources. Therefore, in addition to performance, the computational cost is also a crucial enabling factor [42]. And researchers have investi-

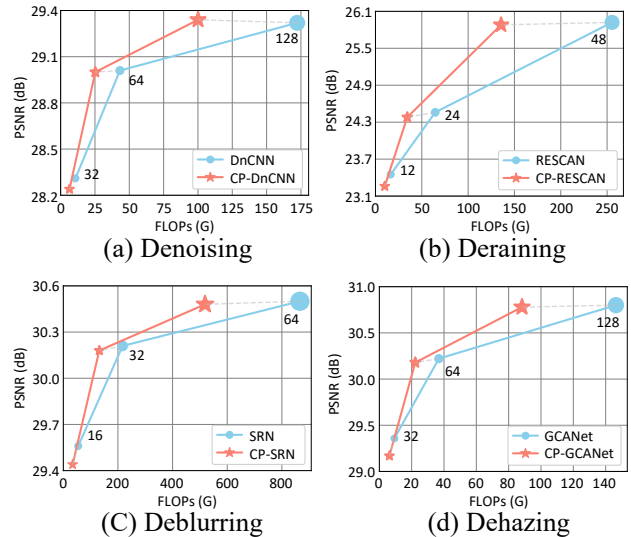


Figure 1. Our ClassPruning can achieve comparable performance and reduce approximately 40% computational costs under different network widths for various image restoration tasks.

gate various methods such as knowledge distillation [16], quantization [19, 67], designing efficient model architecture [17] and pruning [26, 50] to speed up DNNs. However, these methods usually obtain a static network applied to all input samples, which limits the model representation capability, as the diverse demands for network parameters and capacity from different instances are neglected. Dynamic networks, as opposed to static ones, are proposed to adapt their structures or parameters to the input during inference to enjoy favorable properties absent in static models. It uses lightweight networks to deal with easy samples and complex networks to process hard ones, thus reducing the average computational cost. Generally, dynamic networks build a model ensemble through a cascaded [45] or parallel [20] structure and selectively activate the models conditioned on the input, allocating network with appropriate computational cost to each sample. However, the vast network capacity and low inference cost of dynamic networks come at the cost of increased parameters [23, 37], which makes it challenging to deploy to edge devices.

[†]Equal contribution.

We note that pruning is a common technique that discards redundant components to obtain a slimmer network with comparable performance [8, 9, 36], which can be categorized into unstructured pruning and structured pruning. Unstructured pruning removes individual weights at any location and can achieve a high compression ratio [12, 13]. However, the irregular sparsity patterns of weight tensors lead to poor utilization of current vector processing architectures [50]. By contrast, structured pruning removes predetermined structures, such as block [48] and kernel [43, 50], which can better utilize processor resources but fail to maintain accuracy. Recently, $N:M$ fine-grained structured pruning [34, 66] has emerged as a better alternative to combine both the advantage of unstructured pruning and structured pruning. Here, the $N:M$ sparsity means that at most N weights are non-zero for every continuous M weight. Such constraint allows the pruned network to be accelerated on modern hardware [34]. Moreover, we observe that high pruning ratio networks can still well restore lightly degraded images while highly degraded images require low pruning ratio networks to process, as shown in Figure 2. Therefore, we believe $N:M$ fine-grained structured pruning is a sweet solution to marry dynamic networks.

In this paper, we perform dynamic $N:M$ structured pruning on networks based on the input, aiming to reduce the average computational cost while introducing negligible parameters and maintaining performance. We propose a new image restoration pipeline named ClassPruning, which assigns networks with different pruning ratios to images with varying restoration difficulties. The pipeline consists of two parts: Classifier Module and Restoration Module. The Classifier Module is a lightweight classification network that classifies the degraded image into a specific class based on its restoration difficulty. And the Restoration Module is an image restoration network on which we perform dynamic $N:M$ structured pruning to obtain the sparse networks with different capacities. However, training a dynamic pruning network is not a trivial task, so we propose an improved training strategy. We first introduce entropy loss and cost loss to enable the network to trade off performance and efficiency. And we also use variable BatchNorm [18] and SR-STE [66] to stabilize training and improve performance. Finally, we propose a three-stage training scheme: we first pre-train the Classifier Module using pseudo labels, then fix the Classifier Module and only optimize the Restoration Module, and finally finetune the two parts simultaneously end-to-end until convergence. We conducted experiments on several representative image restoration networks, *i.e.*, DnCNN [64] for denoising, RESCAN [27] for deraining, SRN [44] for deblurring and GCANet [4] for dehazing. As shown in Figure 1, ClassPruning could help these restoration networks save approximately 40% of computational cost while maintaining comparable performance.

2. Related Work

Image Restoration. In recent years, learning-based methods [59–61, 64, 65] are rapidly developing and achieving more promising results in various image restoration tasks. DnCNN [64] pioneered using convolution neural networks to handle different levels of Gaussian noise. RESCAN [27] builds a multi-stage architecture to obtain excellent deraining results. SRN [44] explores a multi-scale network for boosting image deblurring performance. And GCANet [4] proposed a gated contextual aggregation network to predict the haze-free image. Despite the remarkable success, most models are complex and require huge computational resources, thus limiting their applications. So we do not aim to design a complicated network but propose a novel image restoration pipeline that reduces models’ computational cost while introducing negligible parameters and maintaining performance via dynamic $N:M$ structured pruning.

Dynamic Networks. Compared to static models, which fix computational graphs and parameters once trained, dynamic networks adjust their structures or parameters to different inputs [3, 25, 47, 52, 53]. Due to its property of assigning different capacity networks to varying inputs, researchers have built dynamic networks through dynamic depth [11, 46], dynamic width [25, 57] and dynamic routing [23, 30] to reduce the models’ average computational cost. Although these methods accelerate models, they often introduce many parameters, making models burdensome and unfriendly to devices with limited memory storage. Therefore, in this paper, we are looking for a dynamic network that adjusts its network capacity based on the image restoration difficulties, which introduces negligible parameters and is hardware friendly.

Network Pruning. Removing unnecessary components of deep neural networks is a promising direction to compress and accelerate models [14, 15, 32, 56]. In addition to structured pruning [8, 13, 40] and unstructured pruning [15, 26, 31], recent works [34, 36, 66] have proposed $N:M$ fine-grained structured pruning as a better alternative that has high efficiency and lossless performance as well as is hardware friendly. Nvidia [34] first presents the design and behavior of Sparse Tensor Cores supported by Ampere GPU architecture to exploit a 2:4 sparsity pattern and describe a simple workflow for training sparse networks to maintain accuracy. Then, SR-STE [66] is proposed to be a simple yet universal recipe for training a $N:M$ sparse neural network from scratch. And SLS [36] introduce a layer-wise $N:M$ sparsity search framework to obtain an efficient image restoration network. Unlike previous works that proposed a training strategy to obtain a high-performance static sparse network, this paper attempts to perform dynamic $N:M$ structured pruning on base restoration models to obtain sparse subnetworks with different capabilities for processing images with varying restoration difficulties.

3. Method

3.1. Observation

We first illustrate our observations on images with different restoration difficulties. Specifically, we perform $N:M$ pruning [34] on DnCNN [64] with different sparsity ratios to obtain varying capacity models for blind Gaussian denoising tasks. From the results shown in Figure 2, we find that images with low noise levels can still be restored well by DnCNN with a 75% sparsity ratio. In contrast, only the unpruned model yields promising restored results for images with high noise levels. Such a finding inspires us to preserve the whole ability of the network and perform $N:M$ pruning on the neural network dynamically according to restoration difficulties of input images, thus achieving a satisfying efficiency and performance tradeoff. Note that such a method introduces only a few parameters so as not to lead to a burdensome model; instead, the $N:M$ fine-grained structured pruning makes the model hardware friendly.

3.2. Network Architecture

Our proposed ClassPruning is a novel image restoration pipeline, as shown in Figure 3, which consists of two parts: Classifier Module and Restoration Module. The Classifier Module classifies the input into L classes, while the Restoration Module can be an arbitrary image restoration network on which we perform $N:M$ fine-grained structured pruning with different sparsity ratios to obtain L branches $\{f_R^i\}_{i=1}^L$ for dealing with different inputs. Specifically, we first feed the degraded image y into the Classifier Module to generate the probability vector $[p_1(y), \dots, p_L(y)]$ of restoration difficulty. Then we determine which sparse subnetwork to be sampled based on the index of the maximum probability value $i = \arg \max_i p_i(y)$. Finally, we handle the input using the i -th sparse network of the Restoration Module.

Classifier Module. The Classifier Module aims to identify the restoration difficulty of the input degraded images efficiently. Thus, we design a lightweight classification network to minimize the additional introduced computational cost and parameters, which contains four convolutional blocks (Conv-BatchNorm [18]-ReLU [10]), an global average pooling layer [29], and a fully-connected layer. The convolutional blocks are responsible for image local features extraction, the global average pooling layer aggregates global information, and the fully-connected layer outputs the probability vector. And our experiments show that such a simple structure can yield satisfying results.

Restoration Module. The Restoration Module is designed to restore degraded images by sparse subnetworks with different capabilities based on the image restoration difficulty. Unlike previous works [9, 28] of judging the importance of each convolutional kernel and conducting channel-wise pruning, we would like to prune networks at a fine-grained



Figure 2. PSNR and qualitative results of various noise level images obtained by sparse DnCNNs under different $N:M$ pruning ratios. Here we set the $N:M$ to be 1:4, 2:4 and 4:4, as well as the noise levels σ to 15, 25 and 50.

level to keep models' performance. Based on the prediction of the Classifier Module, we dynamically perform $N:M$ structured pruning with different sparsity ratios to obtain varying complexity subnetworks. We set the candidate pruning ratios to be 2:4 and 1:4, indicating 50% and 75% reduction in computational costs, respectively. The two pruned networks, together with the base restoration network, form the three branches of the Restoration Module. In this way, we can restore lightly degraded images with high pruning ratio networks and highly degraded images with low pruning ratio networks, thus speeding the image restoration model up while maintaining performance.

3.3. Training Strategy

Classifier Module. Most datasets for image restoration do not label the degraded images with restoration difficulty, preventing us from directly training the Classifier Module. Therefore, we attempt to label the degraded images with the restoration difficulty class. Considering that the degradation processes of tasks are different, we employ different methods to synthesize degraded images with restoration difficulty classes. For image deblurring, we average the adjacent images y_j and then determine the restoration difficulty class based on the number of fused images:

$$y_i = \sum_{j=1}^{N_i} y_j, \quad (1)$$

where N_i is the number of fused images for the i -th class of restoration difficulty. And for denoising, deraining, and dehazing tasks, we first subtract the clean image x from the degraded image y to obtain the degraded components

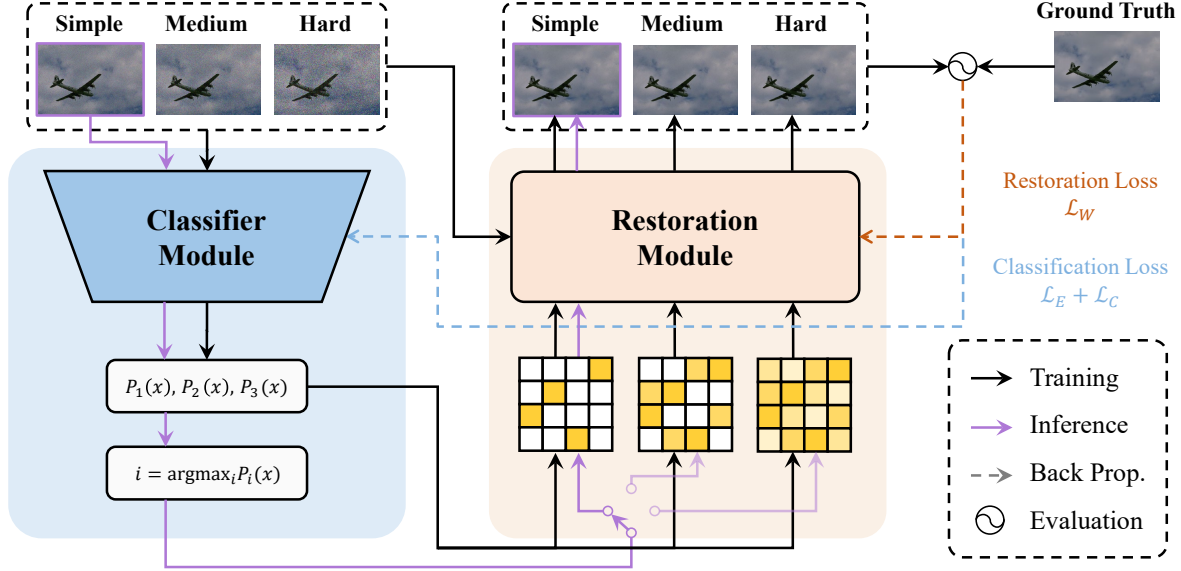


Figure 3. The overview of the proposed ClassPruning, when the number of image restoration difficulty class $M = 3$. Classifier Module: aims to generate the probability vector, Restoration Module: aims to restore the degraded images with corresponding sparse subnetworks.

$R = y - x$. Then we categorize all the R into three classes according to their variance and map each R to the median values of the three classes to satisfy the fact that the same scenario often has different levels of degradation:

$$R_i = \frac{R\sqrt{\text{Var}(R_i^m)}}{\sqrt{\text{Var}[R]}}, \quad (2)$$

where i denotes the class and m means the median value. Finally, we add the new degraded component R_i to the clean image to obtain the labeled degraded image y_i :

$$y_i = x + R_i. \quad (3)$$

So far, we have obtained degraded images with different restoration difficulties, and we can use Cross Entropy (CE) loss to optimize the Classifier Module. However, apart from the degradation level, the restoration difficulty is also related to the content of the degraded images, so the labels obtained with the above method may be biased. Therefore, we use an implicit training approach to finetune the Classifier Module. Specifically, we propose entropy loss L_E and cost loss L_C to train the Classifier Module combined with the Restoration Module. The entropy loss helps the Classifier to have much higher confidence in class with the maximum probability than others, which can accelerate the model convergence and ensure the stability of training:

$$L_E = \sum_{i=1}^L -p_i(y)\log(p_i(y)). \quad (4)$$

Besides, we aim to trade off the effectiveness and efficiency of restoration models. However, when only L_E and reconstruction loss exist, all inputs will be classified as hard samples even though the Classifier Module attains a good initialization by CE loss. To avoid such a bad case, we assign an overhead value C_i to each branch and multiply it with the corresponding probability output by the Classifier Module to form the branch overhead. We sum all the overhead and minimize it to force the input to be classified into the most appropriate restoration difficulty class:

$$L_C = \sum_{i=1}^L p_i(y)C_i. \quad (5)$$

Through subsequent training, we enable the Classifier Module to adaptively classify the images with different restoration difficulties and achieve satisfactory results.

Restoration Module. Our restoration network contains a base network and its sparse versions obtained by dynamic $N:M$ pruning. During testing, the input image only passes through one branch, which is determined by the index of the maximum probability value. In contrast, during training, we allow all degraded images with different restoration difficulties to pass through all L networks and adopt the weighted- L_1 loss L_W to guide the models to reconstruct clean images, where the loss weights of each network are the probability output by the Classifier Module:

$$L_W = \sum_{i=1}^L p_i(y)\|f_R^i(y) - x\|_1. \quad (6)$$

And we weight L_W , L_E and L_C by ω_1 , ω_2 and ω_3 to form the final loss L_F :

$$L_F = \omega_1 L_W + \omega_2 L_E + \omega_3 L_C. \quad (7)$$

Also, we use some strategies to stabilize training and improve performance.

1) *Variable BatchNorm*. The Restoration Module handles images of different restoration difficulties using sparse networks of various capacities. However, when the network consists of BatchNorm layers, using the same BatchNorm layers for all sparse networks leads to severe performance drops due to different pruning ratios altering feature mean and variance. And we solve this problem by using the variable BatchNorm [25], which assigns individual BatchNorm layers for different sparse networks, which are selectively activated depending on the predicted class.

2) *SR-STE*. The pruning operation is non-differentiable, and researchers usually employ Straight-through Estimator (STE) [2] to compensate for sparse neural networks' backpropagation. However, STE only updates the weights that are not set to zero, which might harm our networks' performance since all our subnetworks are ensembled in one model, and individual weight updates are inappropriate. So we use SR-STE [66], which updates all parameters by adding a regularization term to decrease the magnitude of the pruned weights. Experiments show that SR-STE can further improve the model performance.

Training Pipeline. The most intuitive training method is to train the Classifier Module and Restoration Module together from scratch. However, we find this strategy is quite unstable, and even if this model converges, it does not produce promising results. Thus, we propose to train the model in three stages:

- **Stage 1:** Pretrain the Classifier Module with CE loss using the degraded images with pseudo labels;
- **Stage 2:** Fix the parameters of the Classifier Module and train the Restoration Module using L_W ;
- **Stage 3:** Relax all parameters and finetune the whole model with the final loss L_F .

Experimental results show that this scheme can stabilize training and prevent the network from falling into trivial solutions, and somehow boost the model's performance.

3.4. Implementation Details

Considering that we obtain the model in three stages, we first train the Classifier Module using the degraded images with pseudo labels. The mini-batch size is set to 32, and CE Loss is adopted with Adam optimizer [21]. And we use the cosine annealing learning strategy [33] to adjust the learning rate. The total epoch is 200 with the learning rate

from 10^{-3} to 10^{-6} . Then, we fix the Classifier Module and optimize the Restoration Module using L_W with Adam optimizer. The training epoch is 500 with the learning rate from 10^{-4} to 10^{-6} . In the last stage, we relax all the parameters and train the whole model using L_F with Adam optimizer, and the learning rate decays from 10^{-5} to 10^{-7} for 500 epochs. For fair comparisons, we train all the base models for 1,000 epochs with the learning rate from 10^{-4} to 10^{-7} . More details on training protocols are presented in the supplementary material.

4. Experiment

We evaluate our proposed ClassPruning on four different image restoration tasks: (a) image denoising, (b) image deraining, (c) image deblurring, and (d) image dehazing.

4.1. Datasets

Image Denoising. For gaussian image denoising, we follow [5, 64] to use 400 images of size 180×180 for training and BSD68 [41] for testing. Noisy images are generated by adding additive white Gaussian noise with noise level σ to clean images, and we set σ to be 15, 25, and 50 for both training and testing. And for real image denoising, we use 320 high-resolution images of the SIDD dataset [1] to train our model and perform the evaluation on 1280 patches from the SIDD validation set.

Image Deraining. Following [27], we select 700 images from Rain800 [63] to train our model and perform the evaluation on the remaining 100 images, named Test100, for testing. Also, we use Rain100H [54] as the testing dataset to evaluate our model. Note that the PSNR/SSIM scores are computed on the RGB channels instead of the Y channel.

Image Deblurring. Consistent with prior works [35, 44], we use the GoPro [35] dataset for training our model. It contains 2,103 blurry sharp image pairs for training and 1,111 for validation. We also use Kohler dataset [22] for evaluation, which consists of 4 images, and each image is blurred with 12 different kernels.

Image Dehazing. Prior work [24] proposes an image dehazing benchmark RESIDE, which consists of large-scale training and testing hazy image pairs synthesized from depth and stereo datasets. We leverage the RESIDE's Indoor Training Set for training, which contains 1399 clean images and 13990 hazy images generated by corresponding clean images. And we evaluate the models' performance on Synthetic Objective Testing Set (SOTS), which contains 500 indoor images and 500 outdoor ones.

4.2. Comparison with Base Models

To demonstrate the effectiveness and generalization of the method, we use ClassPruning to speed up some representative networks for various image restoration tasks.

Table 1. Comparison between the base models and ClassPruning networks on denoising, deraining, deblurring, and dehazing tasks. The CP-Model means the model is obtained using our proposed ClassPruning, where Model corresponds to the specific model name.

| Methods | BSD68 | | | | | SIDD | | | |
|----------|---------------|---------------|---------------|----------------|---------|-------|-------|----------------|---------|
| | $\sigma = 15$ | $\sigma = 25$ | $\sigma = 50$ | FLOPs | #Params | PSNR | SSIM | FLOPs | #Params |
| DnCNN | 31.63 | 29.18 | 26.24 | 87.28G (100%) | 0.668M | 38.43 | 0.910 | 87.58G (100%) | 0.671M |
| CP-DnCNN | 31.59 | 29.17 | 26.26 | 50.88G (58.3%) | 0.754M | 38.38 | 0.908 | 53.33G (60.9%) | 0.758M |

| Methods | Test100 | | | | Rain100H | | | |
|-----------|---------|-------|----------------|---------|----------|-------|----------------|---------|
| | PSNR | SSIM | FLOPs | #Params | PSNR | SSIM | FLOPs | #Params |
| RESCAN | 24.46 | 0.838 | 64.50G (100%) | 0.589M | 25.71 | 0.832 | 64.50G (100%) | 0.589M |
| CP-RESCAN | 24.38 | 0.838 | 36.18G (56.1%) | 0.672M | 25.60 | 0.830 | 34.31G (53.2%) | 0.672M |

| Methods | GoPro | | | | Kohler | | | |
|---------|-------|-------|---------------|---------|--------|-------|---------------|---------|
| | PSNR | SSIM | FLOPs | #Params | PSNR | SSIM | FLOPs | #Params |
| SRN | 30.21 | 0.933 | 217.2 (100%) | 10.25M | 26.70 | 0.835 | 217.2 (100%) | 10.25M |
| CP-SRN | 30.18 | 0.932 | 131.8 (60.7%) | 10.33M | 26.71 | 0.834 | 132.7 (61.1%) | 10.33M |

| Methods | RESIDE-IN | | | | RESIDE-OUT | | | |
|-----------|-----------|-------|---------------|---------|------------|-------|---------------|---------|
| | PSNR | SSIM | FLOPs | #Params | PSNR | SSIM | FLOPs | #Params |
| GCANet | 30.21 | 0.979 | 36.82 (100%) | 0.702M | 30.36 | 0.963 | 36.82 (100%) | 0.702M |
| CP-GCANet | 30.17 | 0.977 | 22.24 (60.4%) | 0.785M | 30.35 | 0.959 | 21.68 (58.9%) | 0.785M |

Table 2. Comparison with different dynamic approaches. Multi-Width and Multi-Depth are formed by multiple independent networks with different widths and depths. Channel-Skip and Layer-Skip are obtained by skipping layers and channels of the network.

| Method | BSD68 | | | | |
|-------------------|---------------|---------------|---------------|--------|---------|
| | $\sigma = 15$ | $\sigma = 25$ | $\sigma = 50$ | FLOPs | #Params |
| Multi-Width [7] | 31.47 | 29.15 | 26.23 | 50.77G | 1.251M |
| Multi-Depth [37] | 31.60 | 29.17 | 26.27 | 52.11G | 1.272M |
| Channel-Skip [25] | 31.38 | 29.03 | 26.21 | 50.71G | 0.754M |
| Layer-Skip [51] | 31.42 | 29.08 | 26.24 | 51.58G | 0.754M |
| Ours | 31.59 | 29.17 | 26.26 | 50.88G | 0.754M |

Specifically, we use DnCNN [64], RESCAN [27], SRN [44] and GCANet [4] for denoising, deraining, deblurring and dehazing, respectively. Training and testing follow the strategy described above, and results are summarized in Table 1. In summary, ClassPruning helps models obtain comparable performance to the base networks and accelerate all base models approximately 1.67 times (40% FLOPs reduction) by introducing only a few parameters, mainly belonging to the Classifier Module. Also, we find that the reduction of FLOPs is correlated with the restoration task and the test dataset. With comparable performance, the Kohler dataset in the deblurring task is the most difficult, reducing only 39% FLOPs, while the Rain100H dataset in the deraining task is the easiest, reducing 45% FLOPs.

4.3. Comparison with Other Dynamic Networks

We compare ClassPruning with other dynamic networks on the denoising task to demonstrate the effectiveness of our method. And here, we adopted four different dynamic networks: Multi-Width [7], Multi-Depth [37], Channel-

Skip [25] and Layer-Skip [51]. The first two selectively execute one of the multiple independent candidate networks with different depths and widths, respectively. And the last two skip the execution of intermediate layers and channels, respectively. The results are shown in Tabel 2, and we can see that our method outperforms most dynamic approaches, especially the channel-skip, which performs channel-wise structured pruning. We also found that dynamic networks ensembling all the subnetworks in one model are more challenging to optimize than independent subnetworks, and our training strategy could be a good solution. Although our method is slightly inferior to the multi-depth dynamic approach, it is worth noting that ClassPruning introduces fewer parameters, *i.e.* more lightweight, and the $N:M$ sparsity pattern makes our method more friendly to hardware.

4.4. Analysis

Visualization. Figure 4 shows some samples of results obtained by sparse models with different capabilities, and the purple box indicates the branch selected by our Classifier Module. We can see that lightly degraded images can be restored well by sparse networks with high pruning ratios, and only minor improvements are achieved with more complex models. However, when we employ sparse networks with high pruning ratios to handle highly degraded images, the performance drops dramatically and unsatisfying results are produced. Also, it can be seen that our method appropriately assigns networks with different capacities to images with varying restoration difficulties, thus reducing the average computational cost while maintaining performance.

Training Strategy. We obtained the restoration models by training with our proposed strategy and from scratch, re-

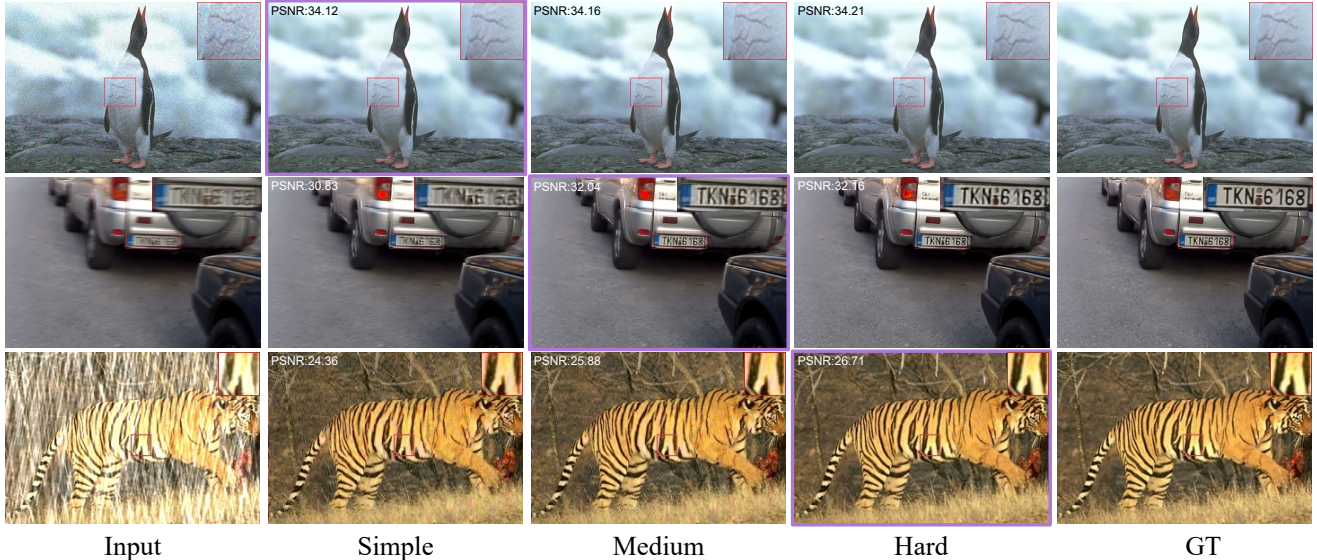


Figure 4. Visual samples obtained by sparse networks with different capabilities. The purple outer box corresponds to the difficulty class predicted by our Classifier Module.

Table 3. Comparison between training from scratch (\dagger) and training with our proposed strategy. Note that we train from scratch multiple times and select the best results due to its instability.

| Methods | BSD68 | | | FLOPs |
|---------------------|---------------|---------------|----------------|----------------|
| | $\sigma = 15$ | $\sigma = 25$ | $\sigma = 50$ | |
| CP-DnCNN \dagger | 31.43 | 29.01 | 26.08 | 51.06G (58.5%) |
| CP-DnCNN | 31.59 | 29.17 | 26.26 | 50.88G (58.3%) |
| Methods | Test100 | | FLOPs | |
| | PSNR | SSIM | | |
| CP-RESCAN \dagger | 24.30 | 0.835 | 37.47G (58.1%) | |
| CP-RESCAN | 24.38 | 0.838 | 36.18G (56.1%) | |
| Methods | GoPro | | FLOPs | |
| | PSNR | SSIM | | |
| CP-SRN \dagger | 30.05 | 0.928 | 130.01 (59.9%) | |
| CP-SRN | 30.18 | 0.932 | 131.83 (60.7%) | |
| Methods | Indoor | | FLOPs | |
| | PSNR | SSIM | | |
| CP-GCANet \dagger | 30.02 | 0.970 | 21.94 (59.6%) | |
| CP-GCANet | 30.17 | 0.977 | 22.24 (60.4%) | |

spectively, to explore the impact of the training strategy on various tasks. It is worth noting that training from scratch is quite unstable and sensitive to the weight ratio of L_C and L_W , leading the Classifier Module to classify all inputs into one restoration difficulty easily; here, we train from scratch multiple times and select the best results. Table 3 shows that our strategy can trade off performance and efficiency better, especially in denoising and deraining tasks. Also, the novel strategy enables our training to be more stable and alleviates the dilemma of being sensitive to losses.

Table 4. Ablation experiments with two optimization methods, variable BatchNorm and SR-STE, on the BSD68 dataset.

| Method | BSD68 | | | FLOPs |
|--------------------------|---------------|---------------|---------------|----------------|
| | $\sigma = 15$ | $\sigma = 25$ | $\sigma = 50$ | |
| vBN \rightarrow BN | 30.02 | 28.14 | 25.58 | 59.69G (68.4%) |
| SR-STE \rightarrow STE | 31.40 | 28.91 | 25.94 | 62.23G (71.3%) |
| Ours | 31.59 | 29.17 | 26.26 | 50.88G (58.3%) |

Variable BN & SR-STE. As mentioned earlier, we employ variable BatchNorm and SR-STE, and here we conducted ablation experiments to investigate their effects as shown in Table 4. The performance drops severely with the same BatchNorm layers for all sparse networks. We believe this is because pruning leads to different statistics of features and variable BatchNorm provides a solution. Also, STE is inferior to SR-STE, which only updates non-zero weights that would harm other sparse networks.

Loss Function. We further investigate the effect of the cost loss L_C and entropy loss L_E by removing them from the loss function. For simplicity, we present the restoration difficulty classification output by the Classifier Module under different losses on BSD68 in Figure 5. We can see that, without L_C , the Classifier Module converges quickly; however, it assigns all degraded images to the hard class, which is a bad local minimum for optimization. And when we remove the L_E , the Classifier Module still classifies all inputs into one class, but the classified class is sensitive to the weight ratios of L_W and L_C . Here we present the probability curve by directly removing the L_E from the baseline. We also only use L_W to train our model and find that the

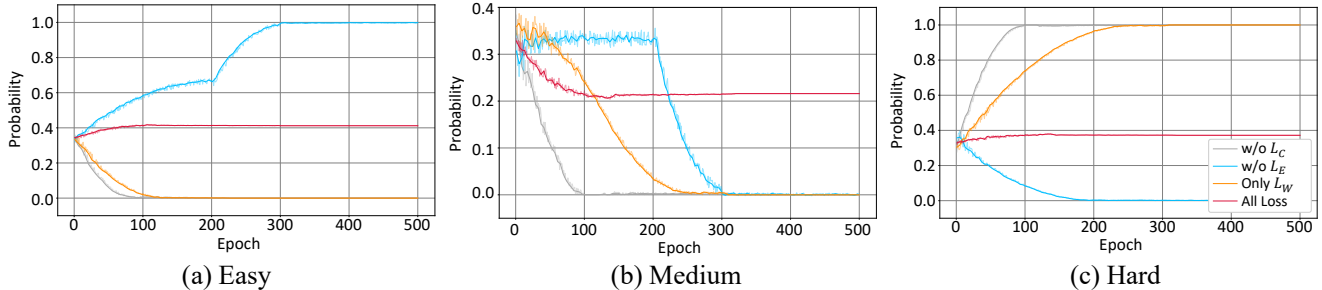


Figure 5. Training probability curves comparison of ClassPruning with various losses on the BSD68 dataset.

Table 5. Ablation experiments of performance and computational cost with different network widths on the denoising task.

| Width | Model | BSD68 | | SIDD | |
|-------|----------|-------|----------------|-------|----------------|
| | | PSNR | FLOPs | PSNR | FLOPs |
| 16 | DnCNN | 27.77 | 5.520G (100%) | 37.08 | 5.580G (100%) |
| | CP-DnCNN | 27.68 | 3.320G (60.2%) | 35.62 | 3.930G (69.1%) |
| 32 | DnCNN | 28.31 | 21.90G (100%) | 37.54 | 22.04G (100%) |
| | CP-DnCNN | 28.24 | 13.01G (59.4%) | 37.06 | 14.37G (63.8%) |
| 64 | DnCNN | 29.01 | 87.28G (100%) | 38.43 | 87.58G (100%) |
| | CP-DnCNN | 29.00 | 50.88G (58.3%) | 38.38 | 53.33G (60.9%) |
| 128 | DnCNN | 29.32 | 348.5G (100%) | 38.77 | 349.1G (100%) |
| | CP-DnCNN | 29.34 | 202.5G (58.1%) | 38.78 | 208.8G (59.8%) |
| 256 | DnCNN | 29.52 | 1,393G (100%) | 38.90 | 1,394G (100%) |
| | CP-DnCNN | 29.55 | 806.4G (57.9%) | 38.87 | 812.7G (58.3%) |

probability curve is similar to the loss without L_C but converges more slowly, indicating our proposed L_E could help the model converge faster. And only when the three losses are used together, the Classifier Module can classify input images appropriately in a more stable way.

Network Width. Considering that we perform $N:M$ pruning on the convolution kernel to obtain the different capacity sparse networks, it is essential to evaluate the impact of the number of the convolution kernel *i.e.*, network channel. We conducted the network width ablation study on the denoising task, and Table 5 shows the performance and computational cost comparisons of models with different widths. When the network width is large enough to be over-parameterized, our method can filter the network redundancy sufficiently, reducing more than 40% computational cost while maintaining or exceeding the original DnCNN’s performance. Such a property is quite valuable since many models nowadays are incredibly complex, and our method can effectively speed them up.

Classification Number. An essential concern in ClassPruning is choosing the appropriate classification number to optimally achieve a balance between performance and efficiency. And we conducted experiments to compare several different classification types. Here we name the **1**, **2**, **4** to represent the 1:4, 2:4 and 4:4 fine-grained structured pruning, and the results are shown in table 6. We find

Table 6. Ablation experiments with different restoration difficulty classifications on the BSD68 dataset. We use **1**, **2**, **4** to represent the 1:4, 2:4 and 4:4 fine-grained structured pruning respectively.

| Type | BSD68 | | | | FLOPs |
|----------------------|---------------|---------------|---------------|-------|----------------|
| | $\sigma = 15$ | $\sigma = 25$ | $\sigma = 50$ | Avg | |
| 1 | 31.21 | 28.69 | 25.83 | 28.58 | 21.82G (25.0%) |
| 2 | 31.43 | 28.85 | 25.98 | 28.75 | 43.64G (50.0%) |
| 4 | 31.63 | 29.18 | 26.24 | 29.02 | 87.28G (100%) |
| 1&2 | 31.28 | 28.74 | 25.88 | 28.63 | 29.33G (33.6%) |
| 1&4 | 31.39 | 28.89 | 26.00 | 28.76 | 49.84G (57.1%) |
| 2&4 | 31.62 | 29.18 | 26.26 | 29.02 | 65.54G (75.1%) |
| 1&2&4 | 31.59 | 29.17 | 26.26 | 29.01 | 50.88G (58.3%) |

that when the pruning ratio is relatively high or only one kind of pruning exists, the restoration models’ performance drops severely (*e.g.*, **1**, **2** and **1&2**). However, when we use **2&4** as our classification type, the model performs well, but the computational cost reduction is not attractive enough. Therefore, we choose the classification type, which divides the restoration difficulty into three classes to trade off the computational cost and performance.

5. Conclusion

This paper proposes a general network slimming pipeline named ClassPruning, which could speed up existing learning-based image restoration models by approximately 1.67 times while maintaining performance. The key idea is first to use the Classifier Module to determine the restoration difficulties of the input images. And then, we perform dynamic $N:M$ fine-grained structured pruning on the restoration model based on the predicted restoration difficulty, thus obtaining the corresponding sparse subnetworks to process the input images. Further, we propose a novel training strategy and two additional loss terms to stabilize training and improve performance. Extensive experiments on various tasks and datasets demonstrate that our ClassPruning could save approximately 40% FLOPs while introducing only a few parameters, indicating the effectiveness and generalization of ClassPruning.

References

- [1] Abdelrahman Abdelhamed, Stephen Lin, and Michael S Brown. A high-quality denoising dataset for smartphone cameras. In *CVPR*, 2018. 5
- [2] Yoshua Bengio, Nicholas Léonard, and Aaron Courville. Estimating or propagating gradients through stochastic neurons for conditional computation. *arXiv preprint arXiv:1308.3432*, 2013. 5
- [3] Bohong Chen, Mingbao Lin, Kekai Sheng, Mengdan Zhang, Peixian Chen, Ke Li, Liujuan Cao, and Rongrong Ji. Arm: Any-time super-resolution method. *arXiv preprint arXiv:2203.10812*, 2022. 2
- [4] Dongdong Chen, Mingming He, Qingnan Fan, Jing Liao, Liheng Zhang, Dongdong Hou, Lu Yuan, and Gang Hua. Gated context aggregation network for image dehazing and deraining. In *WACV*, 2019. 2, 6
- [5] Yunjin Chen and Thomas Pock. Trainable nonlinear reaction diffusion: A flexible framework for fast and effective image restoration. *IEEE TPAMI*, 2016. 5
- [6] Sung-Jin Cho, Seo-Won Ji, Jun-Pyo Hong, Seung-Won Jung, and Sung-Jea Ko. Rethinking coarse-to-fine approach in single image deblurring. In *ICCV*, 2021. 1
- [7] David Eigen, Marc’Aurelio Ranzato, and Ilya Sutskever. Learning factored representations in a deep mixture of experts. *arXiv preprint arXiv:1312.4314*, 2013. 6
- [8] Jonathan Frankle and Michael Carbin. The lottery ticket hypothesis: Finding sparse, trainable neural networks. *arXiv preprint arXiv:1803.03635*, 2018. 2
- [9] Xitong Gao, Yiren Zhao, Łukasz Dudziak, Robert Mullins, and Cheng-zhong Xu. Dynamic channel pruning: Feature boosting and suppression. *arXiv preprint arXiv:1810.05331*, 2018. 2, 3
- [10] Xavier Glorot, Antoine Bordes, and Yoshua Bengio. Deep sparse rectifier neural networks. In *AISTATS*, 2011. 3
- [11] Alex Graves. Adaptive computation time for recurrent neural networks. *arXiv preprint arXiv:1603.08983*, 2016. 2
- [12] Yiwen Guo, Anbang Yao, and Yurong Chen. Dynamic network surgery for efficient dnns. *NeurIPS*, 2016. 2
- [13] Song Han, Jeff Pool, John Tran, and William Dally. Learning both weights and connections for efficient neural network. *NeurIPS*, 2015. 2
- [14] Wei He, Meiqing Wu, Mingfu Liang, and Siew-Kei Lam. Cap: Context-aware pruning for semantic segmentation. In *WACV*, 2021. 2
- [15] Yihui He, Xiangyu Zhang, and Jian Sun. Channel pruning for accelerating very deep neural networks. In *ICCV*, 2017. 2
- [16] Geoffrey Hinton, Oriol Vinyals, Jeff Dean, et al. Distilling the knowledge in a neural network. *arXiv preprint arXiv:1503.02531*, 2015. 1
- [17] Andrew G Howard, Menglong Zhu, Bo Chen, Dmitry Kalenichenko, Weijun Wang, Tobias Weyand, Marco Andreetto, and Hartwig Adam. Mobilenets: Efficient convolutional neural networks for mobile vision applications. *arXiv preprint arXiv:1704.04861*, 2017. 1
- [18] Sergey Ioffe and Christian Szegedy. Batch normalization: Accelerating deep network training by reducing internal covariate shift. In *ICML*, 2015. 2, 3
- [19] Benoit Jacob, Skirmantas Kligys, Bo Chen, Menglong Zhu, Matthew Tang, Andrew Howard, Hartwig Adam, and Dmitry Kalenichenko. Quantization and training of neural networks for efficient integer-arithmetic-only inference. In *CVPR*, 2018. 1
- [20] Robert A Jacobs, Michael I Jordan, Steven J Nowlan, and Geoffrey E Hinton. Adaptive mixtures of local experts. *Neural computation*, 1991. 1
- [21] Diederik P Kingma and Jimmy Ba. Adam: A method for stochastic optimization. *arXiv preprint arXiv:1412.6980*, 2014. 5
- [22] Rolf Köhler, Michael Hirsch, Betty Mohler, Bernhard Schölkopf, and Stefan Harmeling. Recording and playback of camera shake: Benchmarking blind deconvolution with a real-world database. In *ECCV*, 2012. 5
- [23] Xiangtao Kong, Hengyuan Zhao, Yu Qiao, and Chao Dong. Classsr: A general framework to accelerate super-resolution networks by data characteristic. In *CVPR*, 2021. 1, 2
- [24] Boyi Li, Wenqi Ren, Dengpan Fu, Dacheng Tao, Dan Feng, Wenjun Zeng, and Zhangyang Wang. Benchmarking single-image dehazing and beyond. *IEEE TIP*, 2018. 5
- [25] Changlin Li, Guangrun Wang, Bing Wang, Xiaodan Liang, Zhihui Li, and Xiaojun Chang. Dynamic slimmable network. In *CVPR*, 2021. 2, 5, 6
- [26] Hao Li, Asim Kadav, Igor Durdanovic, Hanan Samet, and Hans Peter Graf. Pruning filters for efficient convnets. *arXiv preprint arXiv:1608.08710*, 2016. 1, 2
- [27] Xia Li, Jianlong Wu, Zhouchen Lin, Hong Liu, and Hongbin Zha. Recurrent squeeze-and-excitation context aggregation net for single image deraining. In *ECCV*, 2018. 2, 5, 6
- [28] Ji Lin, Yongming Rao, Jiwen Lu, and Jie Zhou. Runtime neural pruning. *NeurIPS*, 2017. 3
- [29] Min Lin, Qiang Chen, and Shuicheng Yan. Network in network. *arXiv preprint arXiv:1312.4400*, 2013. 3
- [30] Lanlan Liu and Jia Deng. Dynamic deep neural networks: Optimizing accuracy-efficiency trade-offs by selective execution. In *AAAI*, 2018. 2
- [31] Zhuang Liu, Jianguo Li, Zhiqiang Shen, Gao Huang, Shoumeng Yan, and Changshui Zhang. Learning efficient convolutional networks through network slimming. In *ICCV*, 2017. 2
- [32] Zechun Liu, Haoyuan Mu, Xiangyu Zhang, Zichao Guo, Xin Yang, Kwang-Ting Cheng, and Jian Sun. Metapruning: Meta learning for automatic neural network channel pruning. In *ICCV*, 2019. 2
- [33] Ilya Loshchilov and Frank Hutter. Sgdr: Stochastic gradient descent with warm restarts. *ICLR*, 2016. 5
- [34] Asit Mishra, Jorge Albericio Latorre, Jeff Pool, Darko Stosic, Dusan Stosic, Ganesh Venkatesh, Chong Yu, and Paulius Micikevicius. Accelerating sparse deep neural networks. *arXiv preprint arXiv:2104.08378*, 2021. 2, 3
- [35] Seungjun Nah, Tae Hyun Kim, and Kyoung Mu Lee. Deep multi-scale convolutional neural network for dynamic scene deblurring. In *CVPR*, 2017. 5

- [36] Junghun Oh, Heewon Kim, Seungjun Nah, Cheeun Hong, Jonghyun Choi, and Kyoung Mu Lee. Attentive fine-grained structured sparsity for image restoration. In *CVPR*, 2022. 2
- [37] Eunhyeok Park, Dongyoung Kim, Soobeom Kim, Yongdeok Kim, Gunhee Kim, Sungroh Yoon, and Sungjoo Yoo. Big/little deep neural network for ultra low power inference. In *international conference on hardware/software codesign and system synthesis*, 2015. 1, 6
- [38] Kuldeep Purohit, Maitreya Suin, AN Rajagopalan, and Vishnu Naresh Boddeti. Spatially-adaptive image restoration using distortion-guided networks. In *ICCV*, 2021. 1
- [39] Xu Qin, Zhilin Wang, Yuanchao Bai, Xiaodong Xie, and Huizhu Jia. Ffa-net: Feature fusion attention network for single image dehazing. In *AAAI*, 2020. 1
- [40] Vivek Ramanujan, Mitchell Wortsman, Aniruddha Kembhavi, Ali Farhadi, and Mohammad Rastegari. What’s hidden in a randomly weighted neural network? In *CVPR*, 2020. 2
- [41] Stefan Roth and Michael J Black. Fields of experts. *IJCV*, 2009. 5
- [42] Christian Szegedy, Vincent Vanhoucke, Sergey Ioffe, Jon Shlens, and Zbigniew Wojna. Rethinking the inception architecture for computer vision. In *CVPR*, 2016. 1
- [43] Zhanhong Tan, Jiebo Song, Xiaolong Ma, Sia-Huat Tan, Hongyang Chen, Yuanqing Miao, Yifu Wu, Shaokai Ye, Yanzhi Wang, Dehui Li, et al. Pcn: Pattern-based fine-grained regular pruning towards optimizing cnn accelerators. In *DAC*, 2020. 2
- [44] Xin Tao, Hongyun Gao, Xiaoyong Shen, Jue Wang, and Jiaya Jia. Scale-recurrent network for deep image deblurring. In *CVPR*, 2018. 2, 5, 6
- [45] Paul Viola and Michael J Jones. Robust real-time face detection. *IJCV*, 2004. 1
- [46] Xin Wang, Fisher Yu, Zi-Yi Dou, Trevor Darrell, and Joseph E Gonzalez. Skipnet: Learning dynamic routing in convolutional networks. In *ECCV*, 2018. 2
- [47] Yulin Wang, Rui Huang, Shiji Song, Zeyi Huang, and Gao Huang. Not all images are worth 16x16 words: Dynamic vision transformers with adaptive sequence length. *arXiv preprint arXiv:2105.15075*, 2021. 2
- [48] Yanzhi Wang, Shaokai Ye, Zhezhi He, Xiaolong Ma, Linfeng Zhang, Sheng Lin, Geng Yuan, Sia Huat Tan, Zhengang Li, Deliang Fan, et al. Non-structured dnn weight pruning considered harmful. *arXiv preprint arXiv:1907.02124*, 2019. 2
- [49] Zhendong Wang, Xiaodong Cun, Jianmin Bao, Wengang Zhou, Jianzhuang Liu, and Houqiang Li. Uformer: A general u-shaped transformer for image restoration. In *CVPR*, 2022. 1
- [50] Wei Wen, Chunpeng Wu, Yandan Wang, Yiran Chen, and Hai Li. Learning structured sparsity in deep neural networks. *NeurIPS*, 2016. 1, 2
- [51] Zuxuan Wu, Tushar Nagarajan, Abhishek Kumar, Steven Rennie, Larry S Davis, Kristen Grauman, and Rogerio Feris. Blockdrop: Dynamic inference paths in residual networks. In *CVPR*, 2018. 6
- [52] Le Yang, Yizeng Han, Xi Chen, Shiji Song, Jifeng Dai, and Gao Huang. Resolution adaptive networks for efficient inference. In *CVPR*, 2020. 2
- [53] Taojiannan Yang, Sijie Zhu, Chen Chen, Shen Yan, Mi Zhang, and Andrew Willis. Mutualnet: Adaptive convnet via mutual learning from network width and resolution. In *ECCV*, 2020. 2
- [54] Wenhan Yang, Robby T Tan, Jiashi Feng, Jiaying Liu, Zongming Guo, and Shuicheng Yan. Deep joint rain detection and removal from a single image. In *CVPR*, 2017. 5
- [55] Tian Ye, Mingchao Jiang, Yunchen Zhang, Liang Chen, Erkang Chen, Pen Chen, and Zhiyong Lu. Perceiving and modeling density is all you need for image dehazing. *arXiv preprint arXiv:2111.09733*, 2021. 1
- [56] Zhonghui You, Kun Yan, Jinmian Ye, Meng Ma, and Ping Wang. Gate decorator: Global filter pruning method for accelerating deep convolutional neural networks. *NeurIPS*, 2019. 2
- [57] Zhihang Yuan, Bingzhe Wu, Guangyu Sun, Zheng Liang, Shiwan Zhao, and Weichen Bi. S2dnas: Transforming static cnn model for dynamic inference via neural architecture search. In *ECCV*, 2020. 2
- [58] Syed Waqas Zamir, Aditya Arora, Salman Khan, Munawar Hayat, Fahad Shahbaz Khan, and Ming-Hsuan Yang. Restormer: Efficient transformer for high-resolution image restoration. In *CVPR*, 2022. 1
- [59] Syed Waqas Zamir, Aditya Arora, Salman Khan, Munawar Hayat, Fahad Shahbaz Khan, Ming-Hsuan Yang, and Ling Shao. Cycleisp: Real image restoration via improved data synthesis. In *CVPR*, 2020. 2
- [60] Syed Waqas Zamir, Aditya Arora, Salman Khan, Munawar Hayat, Fahad Shahbaz Khan, Ming-Hsuan Yang, and Ling Shao. Learning enriched features for real image restoration and enhancement. In *ECCV*, 2020. 2
- [61] Syed Waqas Zamir, Aditya Arora, Salman Khan, Munawar Hayat, Fahad Shahbaz Khan, Ming-Hsuan Yang, and Ling Shao. Multi-stage progressive image restoration. In *CVPR*, 2021. 1, 2
- [62] Hongguang Zhang, Yuchao Dai, Hongdong Li, and Piotr Koniusz. Deep stacked hierarchical multi-patch network for image deblurring. In *CVPR*, 2019. 1
- [63] He Zhang, Vishwanath Sindagi, and Vishal M Patel. Image de-raining using a conditional generative adversarial network. *IEEE TCSVT*, 2019. 5
- [64] Kai Zhang, Wangmeng Zuo, Yunjin Chen, Deyu Meng, and Lei Zhang. Beyond a gaussian denoiser: Residual learning of deep cnn for image denoising. *IEEE TIP*, 2017. 2, 3, 5, 6
- [65] Yulun Zhang, Yapeng Tian, Yu Kong, Bineng Zhong, and Yun Fu. Residual dense network for image restoration. *IEEE TPAMI*, 2020. 2
- [66] Aojun Zhou, Yukun Ma, Junnan Zhu, Jianbo Liu, Zhijie Zhang, Kun Yuan, Wenxiu Sun, and Hongsheng Li. Learning n: m fine-grained structured sparse neural networks from scratch. *arXiv preprint arXiv:2102.04010*, 2021. 2, 5
- [67] Aojun Zhou, Anbang Yao, Yiwen Guo, Lin Xu, and Yurong Chen. Incremental network quantization: Towards lossless cnns with low-precision weights. *arXiv preprint arXiv:1702.03044*, 2017. 1